Experimental and computational studies on the solvent-controlled cluster isomerism of $Ru_3(H)(CO)_9(NPPh_3)$ and related dynamics†

Roberto Pattacini,[a] Giovanni Predieri,[a] Antonio Tiripicchio,*[a] Carlo Mealli*[b] and Andrew D. Phillips[b]

Received (in Cambridge, UK) 14th November 2005, Accepted 30th January 2006
First published as an Advance Article on the web 27th February 2006
DOI: 10.1039/b516137a

The species $Ru_3(H)(\mu_3\text{-}NPPh_3)(CO)_9$ occurs in the solid state as two isomers, characterized either by one capping hydride and three CO bridges (1a) or by one bridging hydride and all terminals COs (1b); key intermediates for the formation, fluxionality and solvent-dependent interconversion of the isomers are highlighted through a DFT MO analysis.

While dynamic cluster rearrangement in solution is not unusual, structurally characterized solid state isomers are rare.[1] Amongst trinuclear species, $Pt_3(\mu\text{-}PPh_2)Ph(PPh_3)_2$ is remarkable in that it exhibits either an open or closed Pt_3 skeleton (depending on the crystallization solvent)[2] and combines both bond stretching[3] and cluster core isomerism. Other examples include $Os_3(CO)_{11}(PR_3)$ (R = *p*-C_6H_4F) which, depending on the solvent, crystallizes in two different forms. Also in this latter case, the connectivity is unchanged, but two adjacent $Os(CO)_4$ fragments are oriented differently.[4]

Here, we document a more articulated and reversible case of solvent-dependent cluster isomerism, which implies a significant coordination rearrangement. The study was prompted by the scarcely explored engagement of the phosphino-imido ligand in clusters. In fact, the R_3PN unit is generally reported for a few polynuclear cubane-like compounds in which the N atom connects three non-bonded metal atoms.[5] Only in $Fe_3(NO)(CO)_7(\mu\text{-}CO)(\mu_3\text{-}NPPh_3)$, does the ligand cap a triangle of bonded metal atoms.[6]

The reaction of $Ru_3(CO)_{12}$ with an excess of $Ph_3P{=}NSiMe_3$ under pyrolytic conditions (*i.e.* reduced pressure) leads to a number of products at around 130 °C. After extraction with dichloromethane and by using chromatographic techniques, an air and moisture stable compound of general formula $Ru_3(H)(\mu_3\text{-}NPPh_3)(CO)_9$, **1**, is isolated in 46% yield. The rt ^{1}H NMR spectrum, in a $CDCl_3$ solution, shows a low-field doublet at −15.1 ppm ($^3J(^1H,^{31}P)$ = 1.1 Hz), consistent with the chemical shift of a bridging hydride, while the FTIR spectrum is diagnostic of only terminal carbonyls.†

The X-ray structure of **1**,‡ obtained from crystals prepared by evaporation of a hexane solution, appears surprisingly inconsistent with the spectroscopic data and corresponds to $Ru_3(\mu_3\text{-}H)(\mu_3\text{-}NPPh_3)(\mu\text{-}CO)_3(CO)_6$, **1a** (left side of Fig. 1). In fact, three CO bridges lie within the plane of the almost equilateral Ru_3 triangle. Moreover, the hydride ligand occupies a capping and not a bridging position. The Ru_3 triangle is capped, on the opposite side, by the N atom of the $NPPh_3$ ligand. The cluster's skeleton has quasi C_{3v} symmetry, inconsistent with a propeller-like disposition of the phenyl rings. Consequently, the M–M distances are slightly asymmetric (range 2.791(1)–2.842(1) Å). These and other minor deviations are probably due to intermolecular contacts (as short as 2.68 Å) between some terminal CO ligands and phenyl H atoms. The structure **1a** seems unique since the few other relatable clusters of general formula $[Ru_3(H)(\mu_3\text{-}NR)(CO)_9]^n$ (*n* = 0, +1; R = Ph, SOPhMe) have all terminal COs and a bridging H atom.[7]

The DFT (B3LYP)[8,9] optimized C_{3v} model $\mathbf{1a_m}$ (with PH_3 in place of PPh_3) corresponds to a real minimum in the gas phase. Also, the computed and experimental geometries are rather consistent, as indicated by the distances Ru–Ru [2.799 *vs.* 2.821(2) Å (av.)], Ru–N [2.160 *vs.* 2.181(4) Å (av.)] and N–P (1.586 *vs.* 1.606(3) Å).

The unexpected presence of CO bridges in **1a** suggested performing a micro-FTIR analysis on the crystal used for data collection. The spectrum exhibits a strong absorption at 1814 cm^{-1} in the bridging CO region together with a different pattern for terminal CO ligands.§ Recrystallization of the product from dichloromethane afforded new pale yellow crystals and an X-ray analysis revealed a second isomer which, consistent with the spectroscopic data in solution, formulates as $Ru_3(\mu_2\text{-}H)(\mu_3\text{-}NPPh_3)(CO)_9$, **1b**.¶ In the latter, all the COs are terminal and one bridging hydride is off the Ru_3 plane and bent away from the Ph_3PN unit (by 29.84(2)°). As predictable for a 2e-3c bond, the H-bridged Ru2–Ru3 distance (2.818(1) Å) is about 0.15 Å longer than the other M–M bonds [2.667(1) and 2.659(1) Å]. It is worth

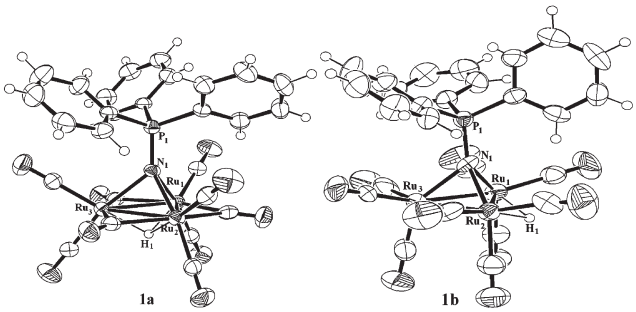

Fig. 1 Views of the crystal structures of isomers **1a** and **1b**. Selected bond distances (Å): **1a**: Ru1–Ru3 2.829(1), Ru1–Ru2 2.842(1), Ru2–Ru3 2.792(2), Ru1–N1 2.196(3), Ru2–N1 2.184(3), Ru3–N1 2.163(3), P1–N1 1.606(3), Ru–H (av.) 1.88(8). **1b**: Ru1–Ru3 2.659(1), Ru1–Ru2 2.667(1), Ru2–Ru3 2.818(1), Ru1–N1 2.097(5), Ru2–N1 2.113(5), Ru3–N1 2.119(5), P1–N1 1.631(5), Ru–H (av.) 1.88(6).

[a]*Dipartimento di Chimica Generale ed Inorganica, Chimica Analitica, Chimica Fisica, Università di Parma, Parco Area delle Scienze 17A, I-43100 Parma, Italy*
[b]*ICCOM, CNR, Via Madonna del Piano 10, 50019, Sesto Fiorentino, Firenze, Italy*

† Electronic supplementary information (ESI) available: Experimental details, FTIR and ^{1}H NMR spectra, crystallographic details and atom labelling schemes. See DOI: 10.1039/b516137a

noticing that the phenyl ring over the H bridge lies perpendicular to the Ru_3 plane, consistent with a quasi C_s molecular symmetry. With respect to **1a**, the three axial COs are more vertical over the Ru_3 plane, but the equatorial ones are pinned towards the Ph_3PN.

Further experiments show a reversible and quantitative convertibility between **1a** and **1b** through different crystallization conditions (Scheme 1). In particular, stabilization of the bridged-H species is enhanced by more polar solvents. However, there is no crystallographic evidence for solvent co-crystallization as a determining factor.

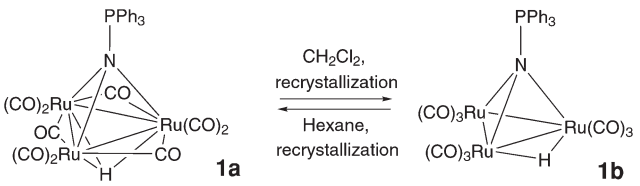

Scheme 1

A DFT optimization confirms that the model $\mathbf{1b_m}$ (with H atoms in place of the phenyl rings) is also a real minimum with a geometry sufficiently consistent with the experimental one. Thus, the H-bridged 2e-3c Ru–Ru bond is elongated with respect to the other two (2.87 *vs.* 2.72 Å) and the hydride is pinned to the Ru_3 triangle at an angle of about 45°. Since the energy of $\mathbf{1b_m}$ is only 3.8 kcal mol^{-1} higher than that of $\mathbf{1a_m}$, both isomers could be present in solution. Although no transition state for their interconversion could be optimized, an effective kinetic barrier may be present. Given the apparent influence of the solvent, four single point calculations (COSMO method[10]) were carried out to mimic the effects of solvents with different polarities on the gas phase species $\mathbf{1a_m}$ and $\mathbf{1b_m}$.

As shown in Scheme 2, the increase in stabilization of about 6 kcal mol^{-1} for $\mathbf{1a_m}$ in heptane (more computationally applicable) is the same as that for $\mathbf{1b_m}$ in CH_2Cl_2. The effects are halved if the solvents are switched. The evident trend is that the CO-bridged cluster is definitely more stable in non-polar solvents, whereas the energy difference becomes insignificant with increasing polarity. Accordingly, the dipole moment (6.08 and 7.32 D for $\mathbf{1a_m}$ and $\mathbf{1b_m}$, respectively) seems to be the discriminating factor for crystallization, even if no specific solvation effect can be highlighted by a method based on a continuous dielectric medium. Further ^1H, ^{31}P and ^{13}C NMR (in the temperature range 213–313 K) and FTIR experiments (see ESI†) confirm that, in solution of either solvent, the only detectable species is **1b**, whereas **1a** is not observed even in hexane from which it crystallizes. Other conformations such as

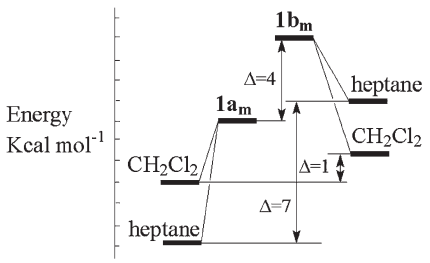

Scheme 2

that with a μ_3 capping hydride could not be confirmed by the ^1H NMR spectrum (expected signal at *ca.* −21 ppm[11]), but it cannot be excluded that this species forms as an intermediate during a rapid fluxional process in solution, thus allowing for the exchange of the H-bridge between the three Ru–Ru bonds. This point is corroborated by the optimization of the key intermediate $\mathbf{1c_m}$ (not a transition state!), which features a capping hydride and all terminal CO ligands (see Scheme 3). The gas phase $\mathbf{1c_m}$ lies 5.7 kcal mol^{-1} above $\mathbf{1b_m}$ but, in CH_2Cl_2, the species is stabilized by as much as 9.9 kcal mol^{-1} (*vs.* the only 6 kcal mol^{-1} of $\mathbf{1b_m}$), so that the fluxional process can be even more facile.

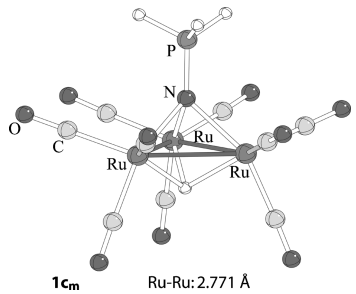

Scheme 3

The situation might be different in heptane, where $\mathbf{1c_m}$ is stabilized by only −4.08 kcal mol^{-1}. This suggests a further key role for **1c**, as an intermediate also for the transformation **1b** → **1a**. This implies a simple merry-go-round mechanism for the carbonyls in the step **1c** → **1a**. According to the Le Chatelier principle, the crystallization from non-polar solvents can shift the equilibrium towards **1a**.[12] A very rapid process may also prevent the detection of **1a** in solution through any spectroscopic means. On the other hand, dissolution of **1a** in polar solvents shifts again the equilibrium towards the H-bridged species.

The calculations were also useful to shed some light on the primary products of the pyrolytic reaction. A reasonable hypothesis is that the $NPPh_3^-$ anion, as a six electron donor, replaces three adjacent axial CO ligands of the parent cluster $Ru_3(CO)_{12}$. The accessibility of the anion $[Ru_3(\mu_3\text{-}NPPh_3)(CO)_9]^-$, **2**, is supported by the optimization of the two models $\mathbf{2a_m}$ and $\mathbf{2b_m}$, which differ for having three bridging or all terminal COs, respectively (see upper part of Scheme 4).

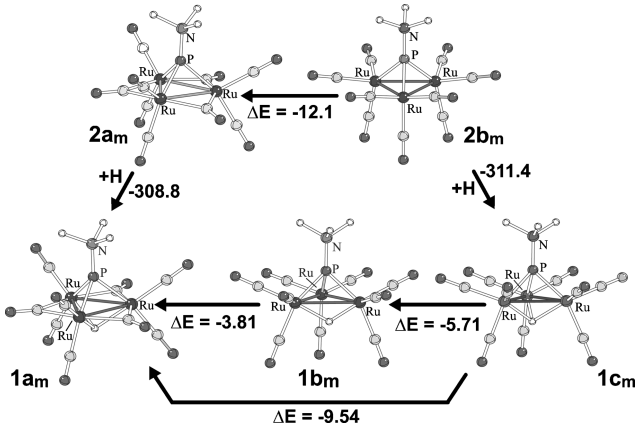

Scheme 4

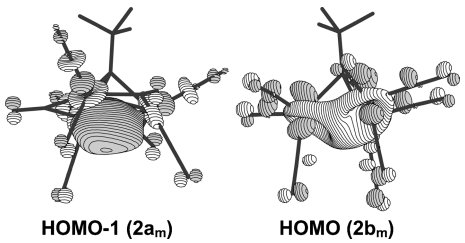

Scheme 5

The CO-bridged species $\mathbf{2a_m}$ is more stable than $\mathbf{2b_m}$ by 12.1 kcal mol^{-1}. This is surprising since none of the parent $M_3(CO)_{12}$ clusters of the group 8 metals has a solid-state structure with three singly bridged M–M bonds. Previous theoretical analysis of the latter systems[13] were limited to the structural dichotomy between non-bridged *vs.* one doubly bridged M–M bond, as found in $Fe_3(CO)_{12}$.

The above computational results prompted an experimental validation. By treating **1** with a strong base (^{t}BuOK or NEt_3), the anion $Ru_3(\mu_3\text{-}NPPh_3)(CO)_9^-$, **2**, is obtained as the deprotonation product. This is proved by the absence of any specific hydride signal in the ^{1}H NMR spectrum. Moreover, the IR spectrum in solution is related to that of the solid-state cluster **1b** and confirms the presence of three bridging COs as in the more stable isomer $\mathbf{2a_m}$. Another interesting observation from Scheme 4 is the significantly larger protonation energy of $\mathbf{2b_m}$ *vs.* $\mathbf{2a_m}$ in the gas phase ($\Delta E_{prot.} = -8$ kcal mol^{-1}) which eventually accounts for the small ΔE between $\mathbf{1a_m}$ and $\mathbf{1b_m}$ (only -3.81 kcal mol^{-1}).

The parent anion **2** (in any isomeric form) is a classic 48e$^-$ species with three single M–M bonds as predicted by the effective atomic number rule.[14] A qualitative MO analysis of the bridged *vs.* non-bridged preferences in the similar M_3L_6 compounds was reported in an early paper by one of us.[15] Importantly, the overall M–M bonding is counterbalanced by electron pair repulsions between the filled non-bonding levels of each metal (t_{2g}-like orbitals in this case).[13,16] The effect is partially relieved in **2a** by the CO bridges, which favour a better metal back-donation. The fact that the parent cluster $Ru_3(CO)_{12}$ has no CO bridges is an indication that three axial COs, in place of the capping $NPPh_3^-$ anion, avoid an excessive accumulation of electron density at the metals. Also, the basicity of compound **2**, the primary product of the reaction between $Ru_3(CO)_{12}$ and $Ph_3PNSiMe_3$, is sufficient to abstract a proton from the surrounding environment (humidity, silica). In any case, protonation during work-up should occur at the capping position, since the HOMOs of both $\mathbf{2a_m}$ and $\mathbf{2b_m}$ (shown in Scheme 5) are in-pointing *radial* combinations of metal σ hybrids. Although less diffuse below the Ru_3 plane, the HOMO of $\mathbf{2b_m}$ lies higher in energy (by about 3.8 kcal mol^{-1}), hence is more basic.

Support for the formation of $\mathbf{1c_m}$ is not only provided by its greater protonation energy, but also by the presence of stronger Ru–H bonds (1.90 *vs.* 1.93 Å, in $\mathbf{1c_m}$ and. $\mathbf{1a_m}$, respectively) as well as by the more hydridic charge of the capping H atom. Even when the hydride is bridging as in $\mathbf{1b_m}$, its role in reducing the intermetallic repulsion should not significantly change, although the electron density is subtracted from a *tangential* rather than a *radial* combination of non-bonding metal orbitals. In conclusion, $\mathbf{1c_m}$ seems to be a very important intermediate both for the fluxional process among three equivalent structures of $\mathbf{1b_m}$ as well as for the interconversion $\mathbf{1b_m} \leftrightarrow \mathbf{1a_m}$.

We thank CINECA for the computing time and usage of programs and Dr Francesco Vizza for some critical NMR measurements.

Notes and references

‡ *Crystal data for* ***1a***: $C_{27}H_{16}N_1O_9P_1Ru_3$, $M = 832.59$, monoclinic $P2_1/n$, $a = 9.153(5)$ $b = 18.797(5)$, $c = 17.026(5)$ Å, $\beta = 72.86(3)^\circ$, $V = 2929(2)$ Å^3, $Z = 4$, $D_c = 1.888$ g cm^{-3}, μ(Mo-Kα) = 1.634 mm^{-1}, $F(000) = 1616$. 5731 reflections were collected with a Bruker SMART1000[17] (Mo-Kα, $\lambda = 0.71073$ Å, $T = 293$ K). The structure was solved by direct methods and refined on F^2 (SHELX97[18]). R_1 and wR_2: 0.031 and 0.039, respectively (420 parameters, 3562 reflections $I > 2\sigma(I)$). CCDC 289256. For crystallographic data in CIF or other electronic format see DOI: 10.1039/b516137a

§ The corresponding CO frequency, calculated for the DFT optimized model $\mathbf{1a_m}$ (see later in the text) is 1801 cm^{-1}.

¶ *Crystal data for* ***1b***: $C_{27}H_{16}N_1O_9P_1Ru_3$, $M = 832.59$, monoclinic $P2_1/c$, $a = 9.359(5)$, $b = 17.665(5)$, $c = 18.101(5)$ Å, $\beta = 100.10(3)^\circ$, $V = 2946(5))$ Å^3, $Z = 4$, $D_c = 1.877$ g cm^{-3}, μ(Mo-Kα) = 1.624 mm^{-1}, $F(000) = 1616$. Identical proceedures, used for **1a**, were followed. Collected reflections: 5036. R_1 and wR_2: 0.041 and 0.044, respectively [285 parameters, 2072 reflections with $I > 2\sigma(I)$]. CCDC 289257. For crystallographic data in CIF or other electronic format see DOI: 10.1039/b516137a

1 See for example: T. Yamaguchi, H. Saito, T. Maki and T. Ito, *J. Am. Chem. Soc.*, 1999, **121**, 10738; D. Adams and J. H. Yamamoto, *J. Cluster Sci.*, 1996, **4**, 643; R. A. Harding and A. K. Smith, *J. Chem. Soc., Dalton Trans.*, 1996, 117; P. Braunstein, C. de Méric de Bellefon, S.-E. Bouaoud, D. Grandjean, J.-F. Halet and J.-Y. Saillard, *J. Am. Chem. Soc.*, 1991, **113**, 5282; M. Mueller, H. T. Schacht, K. Fischer, J. Ensling, P. Guetlich and H. Vahrenkamp, *Inorg. Chem.*, 1986, **25**, 4032.
2 R. Bender, P. Braunstein, A. Dedieu, P. D. Ellis, B. Huggins, P. D. Harvey, E. Sappa and A. Tiripicchio, *Inorg. Chem.*, 1996, **35**, 1223.
3 M.-M. Rohmer and M. Benard, *Chem. Soc. Rev.*, 2001, **30**, 340.
4 V. M. Hansen, A. K. Ma, K. Biradha, R. K. Pomeroy and M. J. Zaworotko, *Organometallics*, 1998, **17**, 5267.
5 U. Riese, N. Faza, W. Massa and K. Dehnicke, *Angew. Chem., Int. Ed.*, 1999, **38**, 528; K. Harms, M. Merle, C. Maichle-Moessmer, W. Massa and M. Krieger, *Inorg. Chem.*, 1998, **37**, 1099; U. Riese, N. Faza, W. Massa, K. Harms, T. Breyhan, P. Knochel, J. Ensling, V. Ksenofontov, P. Gutlich and K. Dehnicke, *Z. Anorg. Allg. Chem.*, 1999, **625**, 1494.
6 U. Eberhardt, G. Mattern and G. Schiller, *Chem. Ber.*, 1998, **121**, 1525.
7 S. Bhaduri, K. Khwaja, N. Sapre, K. Sharma, A. Basu, P. G. Jones and G. Carpenter, *J. Chem. Soc., Dalton Trans.*, 1990, 1313; G. Süss-Fink, G. Rheinwald, H. Stoeckli-Evans, C. Bolm and D. Kaufmann, *Inorg. Chem.*, 1996, **35**, 3081.
8 C. Lee, W. Yang and R. Parr, *Phys. Rev. B*, 1988, **37**, 785.
9 *GAUSSIAN 03 (Revision B.05)*, Gaussian, Inc., Wallingford, CT, 2004 (complete reference in the ESI).
10 F. Eckert and A. Klamt, *AIChE J.*, 2002, **48**, 364.
11 G. Süss-Fink, I. Godefroy, V. Ferrand, A. Neels and H. Stoeckli-Evans, *J. Chem. Soc., Dalton Trans.*, 1998, 515.
12 For a similar case see: N. Burford, T. S. Cameron, K. D. Conroy, B. Ellis, M. Lumsden, C. L. B. Macdonald, R. McDonald, A. D. Phillips, P. J. Ragogna, R. W. Schurko, D. Walsh and R. E. Wasylishen, *J. Am. Chem. Soc.*, 2002, **124**, 14012.
13 E. Hunstock, C. Mealli, M. J. Calhorda and J. Reinhold, *Inorg. Chem.*, 1999, **38**, 5053.
14 D. M. P. Mingos and D. J. Wales, *Introduction to Cluster Chemistry*, Prentice-Hall, Englewood Cliffs, NJ, 1990, p. 93.
15 C. Mealli, *J. Am. Chem. Soc.*, 1985, **107**, 2245–2253.
16 W. Wang, A. J. Carty, E. Sappa, G. Gervasio, C. Mealli, A. Ienco and E. Perez-Carreño, *Inorg. Chem.*, 2000, **39**, 998.
17 *SAINT Software Users Guide*, Bruker Analytical X-ray Systems, Madison, WI,1999; *SMART Software Users Guide*, Bruker Analytical X-ray Systems, Madison, WI,1999; G. M. Sheldrick, *SADABS*, Bruker Analytical X-ray Systems, Madison, WI, 1999.
18 G. M. Sheldrick, *SHELX-97*, University of Göttingen, Germany, 1997.